

# Corrosion behaviour of Fe-9Cr steels in O<sub>2</sub> and CO<sub>2</sub> containing media thick or thin oxide scale?

F. Rouillard, F. Miserque

► **To cite this version:**

F. Rouillard, F. Miserque. Corrosion behaviour of Fe-9Cr steels in O<sub>2</sub> and CO<sub>2</sub> containing media thick or thin oxide scale?. ISHOC 2018, Oct 2018, Matsue, Japan. cea-02338929

**HAL Id: cea-02338929**

**<https://hal-cea.archives-ouvertes.fr/cea-02338929>**

Submitted on 11 Dec 2019

**HAL** is a multi-disciplinary open access archive for the deposit and dissemination of scientific research documents, whether they are published or not. The documents may come from teaching and research institutions in France or abroad, or from public or private research centers.

L'archive ouverte pluridisciplinaire **HAL**, est destinée au dépôt et à la diffusion de documents scientifiques de niveau recherche, publiés ou non, émanant des établissements d'enseignement et de recherche français ou étrangers, des laboratoires publics ou privés.

# Corrosion behaviour of Fe-9Cr steels in O<sub>2</sub> and CO<sub>2</sub> containing media: thick or thin oxide scale ?

Fabien Rouillard and Frederic Miserque

<sup>(1)</sup> CEA, DEN, DPC, SCCME, 91191 Gif sur Yvette, France, Université Paris Saclay  
e-mail: fabien.rouillard@cea.fr

## 1. INTRODUCTION

9-12Cr steels are commonly used for industrial processes involving intermediate to high temperatures. They are of particular interest for heat exchangers since their physical properties (thermal expansion coefficient and thermal conductivity) make them better suited than austenitic steel. Moreover, their low nickel content makes them interesting economically. Recently, their corrosion behaviour have been studied abundantly for potential use in supercritical CO<sub>2</sub> Brayton cycle working at temperature lower than 600 °C. It has been observed that, in industrial CO<sub>2</sub> grade, that is to say containing an amount of impurity (O<sub>2</sub> + H<sub>2</sub>O) usually > 10 ppm, common 9-12Cr steel grades such as T91, T122 or VM12 suffer from fast growing oxide scale coupled to strong carburization whatever the working CO<sub>2</sub> pressure [1]. A corrosion mechanism explaining these coupled oxidation-carburization phenomena has been proposed [1-4]. Recent studies have shown, however, that these same common 9-12 Cr steel grades could form protective Cr rich oxide scale without any carburization of the substrate in research CO<sub>2</sub> grade containing, in that case, very low amount of impurity (usually < 10 ppm) [5, 6]. Moreover, complementary studies suggested that this modification of the corrosion behaviour of 9-12Cr steels in CO<sub>2</sub> depended strongly on the amount of O<sub>2</sub> molecules present as impurities [5, 6]. At atmospheric pressure, with large amount of O<sub>2</sub> in CO<sub>2</sub> (> 100 µbar), 9-12 Cr steels formed fast growing iron oxide scale and carburized whereas with low amount of O<sub>2</sub> in CO<sub>2</sub> (< 10 bar), they form thin protective chromium rich oxide scale and do not carburize. Besides, chemical analyses of the oxide scale built under both environments, pure and impure CO<sub>2</sub>, were carried out immediately after the thermal ramp (550 °C, 2 °C/min) and showed that protective or non-protective corrosion behaviour was already underway before starting the isothermal maintain at 550 °C. Longer exposure times at 550 °C only influenced the oxide thickness but not the oxide composition and oxidation rate.

In order to better understand the corrosion behaviour of 9Cr steel in CO<sub>2</sub> rich gas phase environments and the possible effect of O<sub>2</sub> molecules on the corrosion scale formation, a Gas Phase Analysis technique (GPA) such as named and described in [7] was developed and used at CEA. This innovative device dedicated to the study of gas-solid interaction uses labelled gas molecules and mass spectrometer for analysing the evolution of the gas phase composition. The use of this device combined to the analyses of the corrosion product by multiple techniques such as Raman spectroscopy, SIMS, XPS, SEM and TEM was very powerful to propose an entire story of the steel-gas interaction in CO<sub>2</sub> - O<sub>2</sub> environment.

## 2. EXPERIMENTAL

The Gas Phase Analysis apparatus was composed of three main parts: a “virtually” closed reaction chamber, a gas handling system and a mass spectrometer (MS) placed in an ultra-high vacuum (UHV) chamber. The reaction chamber consisted of a 0.2 m long silica tube and a stainless steel cross. The total volume of the reactor was about 230 cm<sup>3</sup>. Silica tube was chosen as the tube material because it showed negligible reactivity and gas release during the experiments. One end of the tube where the steel sample was positioned was externally heated by a moving furnace positioned on a rail allowing to reach the targeted temperature very fast. One branch of the stainless steel cross part of the reaction chamber was connected to an UHV chamber containing a MS via a leak valve. During experiment, the leak valve was slightly opened to monitor the gas composition in the reaction chamber. The gas was ionized by electron bombardment and the positively charged ions were then directed, using ion optics, to the quadrupole analyzer, where they were separated according to their mass to charge ratio (m/z). In the used condition, a linear response of the partial pressures of all the gas molecules in the UHV chamber and in the reaction chamber could be obtained. The total pressure of the reaction chamber could be measured at room temperature by an absolute capacitive pressure gauge fitted on the stainless steel cross part of the reaction chamber. Another branch of the stainless steel cross part of the reaction chamber was connected to a gas handling system. The gas handling system allowed controlled inlet of high purity isotopic gas molecules in the reaction chamber. In our study, a bottle of high purity <sup>18,18</sup>O<sub>2</sub> and a bottle of high purity <sup>13</sup>C<sup>16,16</sup>O<sub>2</sub> were connected. The isotopic oxygen and carbon composition of these two bottles was chosen in order to distinguish the oxygen transfer to the metallic substrate coming from CO<sub>2</sub> and O<sub>2</sub> molecules and in order to detect any carbon transfer into or out of the <sup>12</sup>C containing steel.

In that work, 0.1 mm thick 9Cr-1Mo foils (EM10 grade) were exposed to pure CO<sub>2</sub>, pure O<sub>2</sub> or CO<sub>2</sub>/O<sub>2</sub> mixture at 550 °C (Table 1). The gas phase composition during the corrosion test was followed by MS and the corrosion products formed on

the sample surface analyzed, ex-situ, by Raman spectroscopy, SIMS, XPS, SEM and TEM.

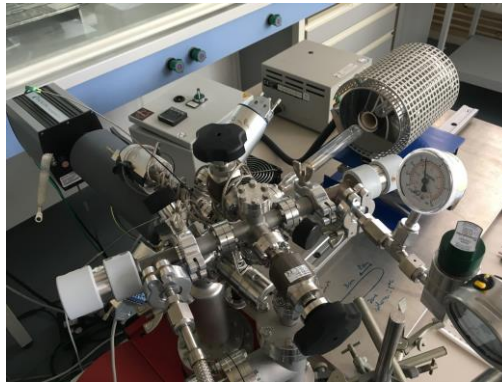


Fig 1. Gas Phase Analysis device

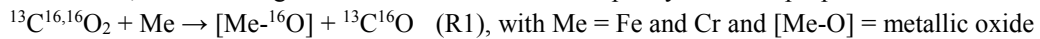
Table 1: Corrosion tests carried out in the GPA facility

Test	P( $^{13}\text{C}^{16,16}\text{O}_2$ ) (mbar)	P( $^{18,18}\text{O}_2$ ) (mbar)	Exposure time (min)	Mass evolution (mg/cm <sup>2</sup> )
9Cr-49CO <sub>2</sub>	49	/	240	-1.3 10 <sup>-3</sup>
9Cr-49CO <sub>2</sub> -1O <sub>2</sub>	49	1	20	1.3 10 <sup>-1</sup>
9Cr-49CO <sub>2</sub> -1O <sub>2</sub>	49	1	240	2.3 10 <sup>-1</sup>
9Cr-1O <sub>2</sub>	/	1	20	3.2 10 <sup>-2</sup>

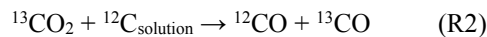
### 3. RESULTS AND DISCUSSION

The evolution of the gas phase composition during exposure of 9Cr sample in 49 mbar of CO<sub>2</sub> at 550 °C for 240 min is shown in Figure 1. It was observed that the  $^{13}\text{C}^{16,16}\text{O}_2$  pressure decreased very slowly and that  $^{13}\text{C}^{16}\text{O}$  formed simultaneously. The total pressure in the reactor staid constant during the test. The rate of formation of  $^{13}\text{C}^{16}\text{O}$  was around 1.10<sup>-3</sup> mbar/min. After test, the colour of 9Cr sample surface changed from bright metallic colour to dark metallic colour. A thin 50 at% chromium – 50 at% iron rich oxide layer formed on the surface (Figure 2) and chromium depletion was observed below it. The formation of Fe<sub>1.5</sub>Cr<sub>1.5</sub>O<sub>3</sub> and/or Fe<sub>1.5</sub>Cr<sub>1.5</sub>O<sub>4</sub> could be proposed.

From these observations, the following oxidation reaction of 9Cr sample by CO<sub>2</sub> was proposed:



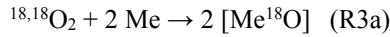
Moreover, GDOES analyses showed slight carbon depletion over a few microns below the oxide layer revealing decarburization in good agreement with the sample mass loss (-10<sup>-3</sup> mg/cm<sup>2</sup>). The proposed decarburization reaction by CO<sub>2</sub> was:



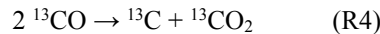
The absence of detection of  $^{12}\text{C}^{16}\text{O}$  molecules formation that reaction (R2) would have induced could be explained by a production rate of  $^{12}\text{C}^{16}\text{O}$  lower than the detection limit of the facility. A decarburization phenomenon by exposure in low pressure pure CO<sub>2</sub> was also observed on mild steel but at a higher rate (not shown in this abstract). To conclude, 9Cr steel exposed to 49 mbar of CO<sub>2</sub> formed a very thin chromium rich oxide layer and decarburized slightly by reaction of Fe, Cr and C with CO<sub>2</sub> molecules.

By adding only 1 mbar of O<sub>2</sub> in 49 mbar of CO<sub>2</sub>, the corrosion behaviour of 9Cr steel changed drastically. After 240 min, the 9Cr sample formed a 1.5 μm thick duplex oxide layer which nature and morphology were as the ones usually observed on 9Cr steel after exposure in industrial grade CO<sub>2</sub> at atmospheric or high pressure [1] : the outer oxide layer was made of Fe<sub>3</sub>O<sub>4</sub> ; the inner oxide layer was made of a complex Fe<sub>3</sub>O<sub>4</sub>-Fe<sub>3-x</sub>Cr<sub>x</sub>O<sub>4</sub> oxide mixture ; the inner/outer layer interface was the initial metallic surface ; the chromium molar concentration in the inner oxide layer was roughly equal to the chromium molar concentration in the metallic substrate (Figure 3 and 4). The gas phase analysis showed that the O<sub>2</sub> molecules ( $^{18,18}\text{O}_2$  and  $^{16,18}\text{O}_2$  coming from the  $^{18,18}\text{O}_2$  bottle) were consumed very fast within the first twenty minutes of exposure. Simultaneously to this consumption, the partial pressure of  $^{13}\text{C}^{16,16}\text{O}_2$  fell down by 3 mbar and, interestingly, the partial pressure of a new CO<sub>2</sub> molecule,  $^{13}\text{C}^{18,16}\text{O}_2$ , rose up to roughly the same quantity, 3 mbar. As a consequence of this reaction process, the CO<sub>2</sub> partial pressure did not evolve during this first twenty minutes time period. Only  $^{18,18}\text{O}_2$  molecules were consumed and isotopic exchange between  $^{18,18}\text{O}_2$  and  $^{13}\text{C}^{16,16}\text{O}_2$  occurred. The proposed scenario to explain these observations would be as follows:  $^{18,18}\text{O}_2$  reacted with 9Cr surface to form  $^{18}\text{O}$  rich oxide. Then, the  $^{13}\text{C}^{16,16}\text{O}_2$  molecules which adsorbed the oxide surface exchanged one of its  $^{16}\text{O}$  atom with the surface oxide  $^{18}\text{O}$  atom to form  $^{13}\text{C}^{16,18}\text{O}_2$

molecules which, then, desorbed and left behind  $^{16}\text{O}$  rich oxide layer. This process was very fast. The isotopic oxygen exchange between  $\text{O}_2$  and  $\text{CO}_2$  molecules via surface oxygen atoms of the oxide layer was proposed since, in most cases, it was shown to be energetically more favourable than direct isotopic exchange between gas molecules [8]. Thus, the exact oxidation reaction of 9Cr steel in presence of  $\text{O}_2$  and  $\text{CO}_2$  molecules could be described according to these two successive reaction steps:



Once all  $\text{O}_2$  molecules were consumed, ie after 20 minutes,  $^{13}\text{C}^{16,16}\text{O}_2$  partial pressure started to decrease and  $^{13}\text{C}^{16}\text{O}$  partial pressure started to increase. The sample oxidized according to reaction (R1). The time dependence of CO production was perfectly parabolic suggesting a diffusion-controlled process. Besides, SIMS analysis of the surface revealed the transfer of  $^{13}\text{C}$  into the metallic substrate below the oxide layer (Fig 6). This carbon enrichment was also detected by GDOES analysis (not shown in this abstract). The carbon transfer into the metallic substrate could be explained by the following Boudouard reaction occurring at the oxide-metal interface:



Thus, in that specific  $\text{CO}_2/\text{O}_2$  environment, it was demonstrated that 9Cr steel corroded fast and carburized. The corrosion mechanism which is proposed in that case is the ‘‘Available Space Model’’ detailed in [1, 3, 4, 9].

Finally, the oxidation behaviour of 9Cr sample in pure  $\text{O}_2$  was studied. In that purpose 9Cr sample was exposed to 1 mbar of  $\text{O}_2$  for 20 min. A duplex oxide scale formed. Surprisingly, the oxide features (microstructure, chromium composition) were very similar to the ones formed in 49 mbar  $\text{CO}_2$  with 1 mbar  $\text{O}_2$  (Fig 7): the oxide was duplex with iron rich oxide in the outer part and iron-chromium rich oxide in the inner part. Nevertheless, its thickness was much lower, about 300 nm to be compared with the 900 nm formed in  $\text{CO}_2\text{-O}_2$  gas mixture for the 20 min period: the oxidation rate of 9Cr steel in 1 mbar of  $\text{O}_2$  was much lower than the one observed in  $\text{CO}_2/\text{O}_2$  binary gas mixture as shown in Fig 8. By analysing more carefully, an interesting observation was that the outer oxide layer formed under 1 mbar of  $\text{O}_2$  was  $\text{Fe}_2\text{O}_3$  instead of  $\text{Fe}_3\text{O}_4$ . Thus, it was proposed that the lower oxidation rate in  $\text{O}_2$  was induced by this  $\text{Fe}_2\text{O}_3$  formation in the outer part of the duplex oxide layer instead of  $\text{Fe}_3\text{O}_4$ . Indeed, it is well known that  $\text{Fe}_2\text{O}_3$  grows at a much lower rate than  $\text{Fe}_3\text{O}_4$  in this temperature domain.

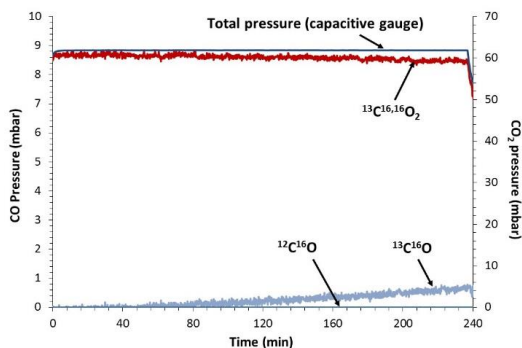


Fig 1. Gas phase composition measured by MS during corrosion test 9Cr-49CO<sub>2</sub>

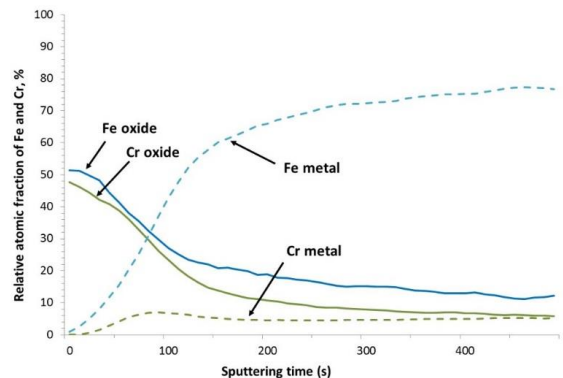


Fig 2. Oxidized and metallic iron and chromium profiles obtained by XPS through 9Cr surface after corrosion test 9Cr-49CO<sub>2</sub>

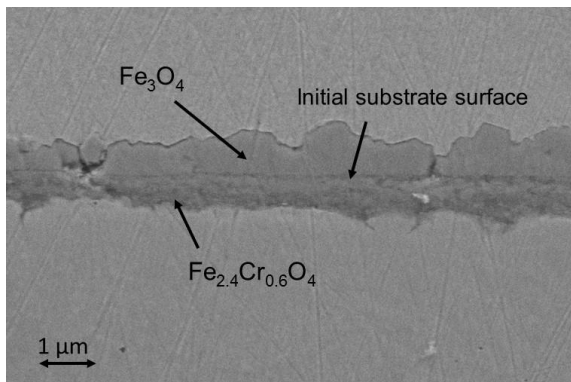


Fig 3. FESEM image of 9Cr cross section after corrosion test 9Cr-49CO<sub>2</sub>-1CO<sub>2</sub>

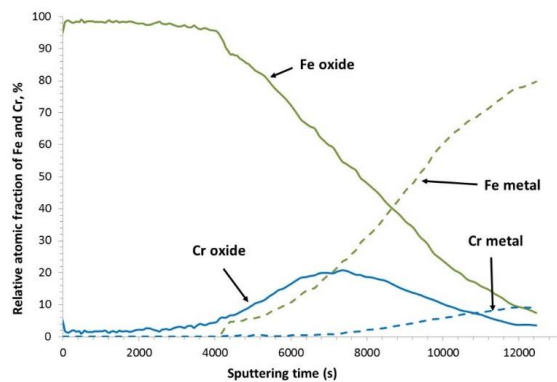


Fig 4. Oxidized and metallic iron and chromium profiles obtained by XPS through 9Cr surface after corrosion test 9Cr-49CO<sub>2</sub>-1O<sub>2</sub>

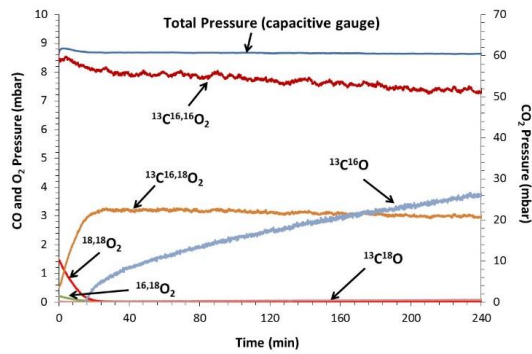


Fig 5. Gas phase composition measured by MS during corrosion test 9Cr-49CO<sub>2</sub>-1O<sub>2</sub>

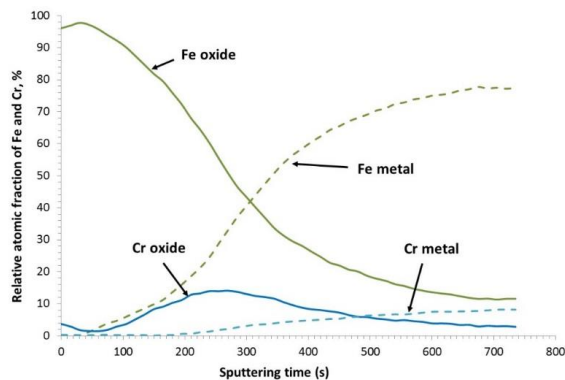


Fig 7. Oxidized and metallic iron and chromium profiles through 9Cr surface after corrosion test 9Cr-1O<sub>2</sub>

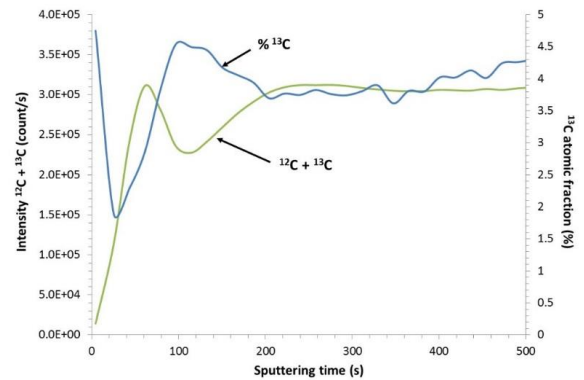


Fig 6. Carbon intensity and <sup>13</sup>C enrichment of C measured through 9Cr surface after corrosion test 9Cr-49CO<sub>2</sub>-1CO<sub>2</sub>

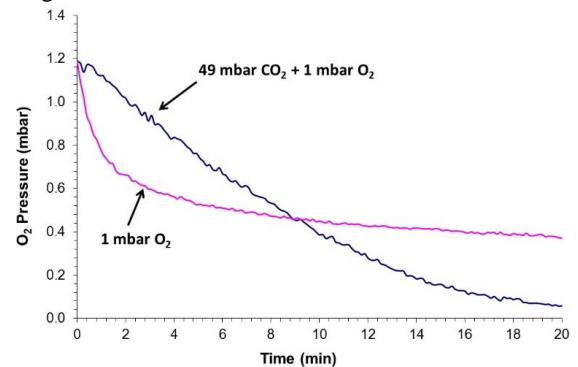


Fig 8. Comparison of the O<sub>2</sub> pressure consumption as a function of time in test 9Cr-49CO<sub>2</sub>-1O<sub>2</sub> and test 9Cr-1O<sub>2</sub>

#### 4. CONCLUSIONS

By using an innovative Gas Phase Analysis device using labelled molecules, mass spectrometer and pressure gauge, it was showed that the corrosion behaviour of 9Cr steel at 550 °C in low pressure CO<sub>2</sub> rich environment depends strongly on the presence of O<sub>2</sub> molecules. First, in pure CO<sub>2</sub>, the steel formed a slow growing Cr rich oxide scale and decarburized slightly. Then, in 1 mbar of O<sub>2</sub>, 9Cr steel formed as well a slow growing oxide layer but its low oxidation rate was likely induced, in that case, by the formation of Fe<sub>2</sub>O<sub>3</sub>. Finally, by adding 1 mbar of O<sub>2</sub> in CO<sub>2</sub>, the corrosion behaviour of 9Cr steel was modified drastically: a fast growing duplex oxide scale formed and strong carburization of the substrate occurred. An oxidation scenario explaining all observed corrosion behaviour of 9Cr steel either in O<sub>2</sub>, in CO<sub>2</sub> or in CO<sub>2</sub>/O<sub>2</sub> binary mixture will be detailed at the conference.

#### References

- [1] F. Rouillard, T. Furukawa, Corrosion of 9-12Cr ferritic-martensitic steels in high-temperature CO<sub>2</sub>, *Corros. Sci.*, 105 (2016) 120-132.
- [2] F. Rouillard, L. Martinelli, Corrosion of 9Cr Steel in CO<sub>2</sub> at Intermediate Temperature III: Modelling and Simulation of Void-induced Duplex Oxide Growth, *Oxid. Met.*, 77 (2012) 71-83.
- [3] F. Rouillard, G. Moine, M. Tabarant, J. Ruiz, Corrosion of 9Cr Steel in CO<sub>2</sub> at Intermediate Temperature II: Mechanism of Carburization, *Oxid. Met.*, 77 (2012) 57-70.
- [4] F. Rouillard, G. Moine, L. Martinelli, J. Ruiz, Corrosion of 9Cr Steel in CO<sub>2</sub> at Intermediate Temperature I: Mechanism of Void-Induced Duplex Oxide Formation, *Oxid. Met.*, 77 (2012) 27-55.
- [5] S. Bouhieda, F. Rouillard, V. Barnier, K. Wolski, Selective oxidation of chromium by O<sub>2</sub> impurities in CO<sub>2</sub> during initial stages of oxidation, *Oxid. Met.*, 80 (2013) 493-503.
- [6] S. Bouhieda, F. Rouillard, K. Wolski, Influence of CO<sub>2</sub> purity on the oxidation of a 12Cr ferritic-martensitic steel at 550°C and importance of the initial stage, *Materials at High Temperature*, 29 (2011) 151-158.
- [7] C. Anghel, Q. Dong, A gas phase analysis technique applied to in-situ studies of gas-solid interactions, *J. Mater. Sci.*, 42 (2007) 3440-3453.
- [8] T. Titani, T. Kiyoura, A. Adachi, An isotopic exchange reaction between oxygen and carbon dioxide on zinc oxide, *Bull. Chem. Soc. Jpn.*, 38 (1965) 2075-+.
- [9] L. Martinelli, C. Desgranges, F. Rouillard, K. Ginestar, M. Tabarant, K. Rousseau, Comparative corrosion behavior of 9Cr-1Mo steel in CO<sub>2</sub> and H<sub>2</sub>O at 550°C : detailed analysis of the inner oxide layer, *Corros. Sci.*, 100 (2015) 253-266.